which contain information about wind speed and wave height were often found to be degraded at these ranges. Nevertheless, the technique can be improved, and better measures of wind and waves are expected, particularly at shorter ranges near 2000 km.

REFERENCES

[1] D. D. Crombie, "Doppler spectrum of sea echo at 13.56 Mc/s," *Nature*, vol. 175, pp. 681–682, 1955.

[2] D. E. Barrick, "First-order theory and analysis of MF/HF/VHF scatter from the sea," *IEEE Trans. Antennas Propagat.*, vol. AP-20, pp. 2–10, 1972.

[3] S. O. Rice, "Reflection of electromagnetic waves from slightly rough surfaces," in *Theory of Electromagnetic Waves*, M. Kline, Ed. New York: Interscience, pp. 351–378.

[4] A. Sommerfeld, *Optics, Volume IV of Lectures on Theoretical Physics*. New York: Academic Press, 1964, 383 pp.

[5] O. M. Phillips, *The Dynamics of the Upper Ocean*. Cambridge: The University Press, 1966, 261 pp.

[6] W. A. Nierenberg and W. H. Munk, "Sea spectra and radar scattering," Institute for Defense Analysis Note N-817, 22 pp, 1972, AD760693.

[7] C. C. Teague, "Bistatic-radar techniques for observing long-wavelength directional ocean-wave spectra," *IEEE Trans. Geoscience Elec.*, vol. GE-9, pp. 211–215, 1971.

[8] E. P. Anderson, "Characteristics of sea reflections at 1.85 Mc," Engineer's Thesis, Stanford University, Stanford, CA, 1957.

[9] A. M. Peterson, C. C. Teague, and G. L. Tyler, "Bistatic-radar observation of long-period, directional ocean-wave spectra with Loran A," *Science*, vol. 170, pp. 158–161, 1970.

[10] C. C. Teague, G. L. Tyler, J. W. Joy, and R. H. Stewart, "Synthetic aperture observations of directional height spectra for 7 s ocean waves," *Nature, Physical Sciences*, vol. 244, pp. 98–100, 1973.

[11] G. L. Tyler *et al.*, "Wave directional spectra from synthetic aperture observations of radio scatter," *Deep Sea Research*, vol. 21, pp. 989–1016, 1974.

[12] C. C. Teague, "In-situ decametric radar observations of ocean-wave directional spectra during the 1974 Norpax 'Pole' experiment: final report," Radioscience Lab., Stanford University, Tech. Rep. SEL-75-003, 1975.

[13] C. C. Teague, G. L. Tyler, and R. H. Stewart, "The radar cross-section of the sea at 1.95 MHz: comparison of in-situ and radar determinations," *Radio Science*, vol. 10, pp. 847–852, Oct. 1975.

[14] D. E. Barrick, J. M. Headrick, R. W. Bogle, and D. D. Crombie, "Sea backscatter at HF: Interpretation and utilization of the echo," *Proc. IEEE*, vol. 62, pp. 673–680, 1974.

[15] R. H. Stewart and J. W. Joy, "HF radio measurement of surface currents," *Deep Sea Research*, vol. 21, pp. 1039–1049, 1974.

[16] J. Wu, "Wind-induced drift currents," *J. Fluid Mechanics*, vol. 68, pp. 49–70, 1975.

[17] K. Hasselmann, "Determination of ocean wave spectra from Doppler radio return from the sea surface," *Nature, Physical Science*, vol. 229, pp. 16–17, 1971.

[18] D. E. Barrick, "Remote sensing of sea state by radar," in *Remote Sensing of the Troposphere*, V. Derr, editor, U.S. Government Printing Office, Chapter 12, 12–1 to 12–46, 1972.

[19] D. L. Johnstone, "Second-order electromagnetic and hydrodynamic effects in high-frequency radio-wave scattering from the sea," Radioscience Lab., Stanford University, Tech. Rep. SEL-75-004, 1975.

[20] J. F. Ward, "Power spectra from ocean movements measured remotely by ionospheric radio backscatter," *Nature*, vol. 223, pp. 1325–1330, 1969.

[21] G. L. Tyler, W. E. Faulkerson, A. M. Peterson, and C. C. Teague, "Second-order scattering from the sea: Ten-meter radar observations of the Doppler Continuum," *Science*, vol. 177, pp. 349–351, 1972.

[22] D. L. Johnstone, "A comparison of theoretical and measured Doppler spectra of sea echoes at 1.95 MHz," submitted to *Radio Science*.

[23] A. E. Long and D. B. Trizna, "Mapping of North Atlantic winds by HF radar sea backscatter interpretation," *IEEE Trans. Antennas Propagat.*, vol. AP-21, pp. 680–685, 1973.

[24] R. H. Stewart and J. R. Barnum, "Radio measurements of oceanic winds at long ranges: an evaluation," *Radio Science*, vol. 10, pp. 853–858, Oct. 1975.

The Statistics of HF Sea-Echo Doppler Spectra

DONALD E. BARRICK, MEMBER, IEEE, AND JACK B. SNIDER, MEMBER, IEEE

Abstract—**Several important statistical properties of the HF sea echo and its Doppler power spectrum, which are useful in optimizing the design of radar oceanographic experiments, are established. First- and second-order theories show that the echo signal (e.g., the voltage) should be Gaussian; this is confirmed with experimental surface-wave data i) by comparison of the normalized standard deviation of the power spectrum at a given frequency with its predicted value of unity, and ii) by cumulative distribution plots of measured spectral amplitudes on Rayleigh probability charts. The normalized standard deviation of the dominant absolute peak amplitudes of the power spectrum (which wander slightly in frequency) are shown from experimental data to be ~ 0.7 for the first-order peaks and ~ 0.5 for the second-order peaks. The autocorrelation coefficient of the power spectra is derived from measured data and interpreted in terms of the spectral peak widths; from this information, the correlation time (or time between independent power spectrum samples) is shown to be ~ 25–50 s for radar frequencies above 7 MHz. All of these statistical quantities are observed to be independent of sea state, scattering cell size, and relatively independent of radar operating frequency. These quantities are then used to establish the statistical error (and confidence interval) for radar remote sensing of sea state, and it is shown, for example, that 14 power spectral samples result in a sample average whose rms error about the true mean is 1.0 dB.**

Manuscript received December 11, 1975; revised July 30, 1976.

The authors are with the U.S. Department of Commerce, National Oceanic and Atmospheric Administration, Environmental Research Laboratories, Boulder, CO 80302.

I. INTRODUCTION

TWO DECADES AGO, Crombie [1] experimentally deduced the physical mechanism responsible for first-order HF sea echo. The unique characteristics of his high-resolution Doppler records led to the conclusion that the dominant spectral peaks resulted from Bragg scatter; i.e., only those ocean wavetrains will backscatter near grazing whose spatial period is exactly one-half the radar wavelength and which move directly toward and/or away from the radar. In later deterministic analyses, Wait [2] confirmed this deduction and showed further that the strength of this first-order echo is proportional to the height of the resonant "Bragg-scattering" ocean waves. These con-

clusions suggested the exciting possibility of employing HF radars (both sky-wave and surface-wave) to measure the ocean waveheight directional spectrum—or "sea state." Recently a number of groups have been investigating the use of such HF radar techniques for remotely sensing ocean surface conditions via the sea-echo Doppler spectrum.

One of the very important properties of the HF sea echo, however, is its random nature. This point is often overlooked because resonant (or Bragg) scatter is such a precisely describable physical phenomenon that many have assumed that a single echo record describes the scattering surface satisfactorily. Since the heights of the Bragg-scattering waves within the radar resolution cell are random variables (in fact, the entire sea-surface height is a random variable best described via the Fourier–Stieltges integral or the Fourier series with random coefficients), the sea echo must also be a random variable. This fact was employed in the analyses of Barrick and Peake [3] and Barrick [4], [5], who showed that to first and second order, the *average* sea-echo Doppler spectrum is related to the *average* sea waveheight directional spectrum evaluated at the required first and second-order Bragg wavenumbers.

All of the suggested methods for extracting sea-state parameters from the sea-echo Doppler spectrum involve the comparison (i.e., division) of one part of the echo spectrum by another part [6], [7]. Failure to note that the sea echo is a random variable will lead to a statistical fluctuation in the desired parameter. Hence, appropriate averaging of each sea-echo feature is necessary before the deduction of the desired mean sea-state descriptor. Since "averaging time" in a practical experiment is not unlimited,[1] the number of independent samples used to approximate the average may in fact be small. Therefore, in order to calculate the accuracy of predicting the desired sea parameter, one must know something about the statistics of the echo, such as the power spectrum variance, correlation time, etc. While it is often customary to assume Gaussian statistics for the scattered electric field, this assumption in many cases remains to be proven. In the microwave region, for example, where the physical mechanism behind near-grazing sea backscatter is considerably more complex than at HF, Trunk [8] has found that the echo voltage distribution in certain cases can be log-normal, while in others it follows the Gaussian (or normal) model.

First, we provide a heuristic theoretical rationale explaining why the complex components of the first- and second-order sea echo are Gaussian random variables. Then we examine the properties of Gaussian processes, in particular, deriving the probability density and the normalized standard deviation of the power for each Doppler frequency spectrum taken as the random variable. Next, we calculate both the normalized standard deviation and the temporal correlation function of the Doppler spectrum from HF suface-wave sea-echo measurements. We compare these experimental results with the theoretical predictions for Gaussian processes (where the latter are available). Finally, we give an example of the use of the derived statistical properties of the sea echo in the analysis/design of an HF radar experiment.

[1] The total observation time is proportional to the coherent integration time multiplied by the number of sequential beam scans times the desired number of samples per radar resolution cell. The coherent integration time is the reciprocal of the required Doppler resolution. The total observation time should not exceed the interval over which the sea is statistically stationary; the latter time may typically vary between 1 and 12 h.

II. Sea Echo and the Gaussian Process

It is often customary to assume that in general random signals (e.g., voltages) are Gaussian because i) the Gaussian model has desirable mathematical properties, making manipulations with it easy, ii) if the signal is synthesized as the sum of several independent events, the Central Limit Theorem states that as the number of events becomes large, the sum signal approaches a Gaussian random variable, iii) wideband spectrally flat random signals after narrowband filtering (such as at the output of a finite Fourier transform) tend to Gaussian under most conditions [9], and conversely, iv) a wideband signal synthesized by the summation of Gaussian random narrowband signals will be Gaussian because linear operations on Gaussian variables produce Gaussian variables [10]. Since one can always find mathematical exceptions to these generalizations, and since the sea-echo spectrum is *not* flat, we will establish separate, independent proofs from the scattering theory to justify the Gaussian assumption.

The conventional method for analyzing HF sea echo employs the classical statistical boundary perturbation approach first set forth by Rice [11]. This technique requires that the surface waveheight be small in terms of the radar wavelength and that the surface slopes be small; both of these conditions are satisfied (in the mean) by the sea surface at HF. By ordering the terms in the scattered field solution according to the above "smallness" parameters, expressions have been derived for the first-order and second-order sea echo [4], [5]. These expressions show that Bragg scatter—the mechanism originally proposed by Crombie [1]—does, in fact, account for the echo.

In the formulation of this theory, the sea surface height is represented by an exponential spatial Fourier series with random complex coefficients $P(m,n)\,(= X(m,n) + iY(m,n))$, where m and n are running indices corresponding to the x and y directions (the latter taken as lying in the mean surface plane). The total sea surface height has been shown by oceanographers [12] to be representable as a Gaussian random variable *to first-order*. The requirement that the sea height be a real quantity means that $P^*(m,n) = P(-m,-n)$ (or $X(-m,-n) = X(m,n)$ and $Y(-m,-n) = -Y(m,n)$). The average sea waveheight directional spectrum $S(\kappa_x,\kappa_y)$, is then defined in terms of these coefficients as

$$\langle P(m,n)P^*(m',n')\rangle = \begin{cases} a^2 S(am,an), & \text{for } m',n' = m,n \\ 0, & \text{for } m',n' \neq m,n \end{cases} \quad (1)$$

where $a \equiv 2\pi/L$, L being defined as the fundamental spatial period of the Fourier series. These first-order height co-

efficients $P(m,n)$ may be taken to be uncorrelated random variables [13]; inasmuch as the waveheight can be considered a spectrally flat process over a nominally wide band of spatial wavenumbers, the random Fourier coefficients can also be taken to be Gaussian [9].

To first order, the backscattered electric field at the receiver is [4]

$$E^{(1)} = KP_{\pm}(m_*,n_*) \exp\{-i[\omega_0 \mp \sqrt{ag(m_*^2 + n_*^2)^{1/2}}]t\} \tag{2}$$

where K is a complex constant which depends upon the propagation loss to the scattering patch, incidence angle, and other fixed factors of the geometry. The quantity ω_0 is the transmitted radian carrier frequency; the Doppler shift of the scattered signal from the carrier,

$$\sqrt{ag(m_*^2 + n_*^2)^{1/2}} \; (\equiv \omega_B),$$

originates as a result of the first-order dispersion relation between the spatial and temporal wavenumbers of a gravity wave, with g being the acceleration of gravity (~ 9.81 m/s^2). Hence, $\kappa_* = a(m_*^2 + n_*^2)^{1/2}$ is the spatial wavenumber of the particular Fourier-series components responsible for the scatter. The theory shows that only a very small number of Fourier-series components can contribute to scatter. These have wavenumbers along and perpendicular to the radar line of sight (for backscatter at grazing incidence) such that $\kappa_{x*} = am_* \approx 2k_0$, and $\kappa_{y*} = an_* \approx 0$, where k_0 is the radar spatial wavenumber ($k_0 = \omega_0/c = 2\pi/\lambda$); these are precisely the required conditions for first-order Bragg scatter, as originally deduced empirically by Crombie.

Equation (2) essentially shows that if $P(m,n)$ is a Gaussian random variable, as assumed in our description of the ocean, then the signal is itself a random variable which is directly proportional to the waveheight coefficient. Since any linear operation on a Gaussian random variable produces another Gaussian random variable, the received signal is therefore itself Gaussian. Hence one has a proof that the first-order sea echo is Gaussian *so long as one can assume that the height of the sea can be represented by a Gaussian random variable to first order.*

To second order, the signal scattered from the sea is [5]

$$E^{(2)} = iK \sum_m \sum_n \Gamma_T(m,n) P_{\pm}(m,n) P_{\pm}(m_* - m, n_* - n) \times \exp\{-i[\omega_0 \mp \sqrt{ag[m^2 + n^2]^{1/2}} \mp \sqrt{ag[(m_* - m)^2 + (n_* - n)^2]^{1/2}}]t\} \tag{3}$$

where K has the same value as in (1), and m_*,n_* are as defined after (2), i.e., a narrow band of numbers satisfying the first-order Bragg-scatter criterion. Equation (3) is actually an expression of second-order Bragg scatter, where one set of the double-interacting ocean waves has spatial wavenumber $\bar{\kappa}_1 = am\hat{x} + an\hat{y}$ and the other has spatial wavenumber $\bar{\kappa}_2 = a(m_* - m)\hat{x} + a(n_* - n)\hat{y}$. The summation over m,n indicates that there is an infinite number of double sets of ocean waves possible which can interact to second order (to first order, only one single set was possible for each Doppler shift). Each double set in turn produces its own echo Doppler shift from the carrier, as seen from the argument of the exponential; in the limit the summations merge into a double integral, and the Doppler spectrum is seen to be a continuous function. The "transfer coefficient" Γ_T has been derived and presented elsewhere [5]; it is a deterministic constant which results from the second-order terms from both the nonlinear boundary condition at the water–air interface (the hydrodynamic contribution) and also from the second-order terms in the nonlinear perturbation expansion of the scattered fields (the electromagnetic contribution).

Writing (3) in this manner expresses the hypothesis that if each of the two different P in each term of the summation is a Gaussian random variable, the second-order scattered field is also a random variable. However, each term of the summation, consisting of a product of two Gaussian random variables, is no longer Gaussian.[2] Nevertheless, many terms of the series of (3) can be seen to contribute to the signal at a given Doppler shift, hence, one can argue by the central limit theorem [13] that the result for each Doppler shift, being the sum of many independent non-Gaussian terms, nonetheless will tend toward Gaussian.

The point of this section was to show from the presently accepted theoretical derivations that the real and imaginary parts of the instantaneous complex signal at each Doppler shift are predicted to be Gaussian random variables. Since the temporal Fourier transform, as obtained from a digital processor at the output of an HF receiver, is nothing more than a weighted sum of the coefficients of the Doppler time series given by (2) and (3), this complex transform at each spectral point should also be Gaussian (i.e., the real and imaginary parts of the Fourier transform have Gaussian probability distributions). Thus, for example, if the Fourier transform is obtained with 0.02 Hz resolution (requiring 50 s of signal data), the complex parts of this transform should be Gaussian random variables. This will be true regardless of the integration time.

This latter fact is often erroneously overlooked by some, who feel that the longer the sample in time (or the larger the basic scatter area in space for a given scatter sample), the "smoother" the signal should be because of "temporal" or "spatial" averaging.[3] It will be shown from experimental data that the components of the complex received signal (in both the first-order and second-order spectral regions) appear in fact to be Gaussian, regardless of the coherent processing time or the size of the scatter area.

[2] The real and imaginary part of each *product* term can be shown to have an exponential probability density function given by $p(U) = \exp\{-|U|/\sigma_1\sigma_2\}/(2\sigma_1\sigma_2)$; $p(V) = \exp\{-|V|/\sigma_1\sigma_2\}/(2\sigma_1\sigma_2)$, where $U = X(m_1,n_1)X(m_2,n_2) - Y(m_1,n_1)Y(m_2,n_2)$ and $V = X(m_1,n_1) \cdot Y(m_2,n_2) + X(m_2,n_2)Y(m_1,n_1)$ are the real and imaginary parts of the product coefficients; $2\sigma_1^2 \equiv a^2S(am_1,an_1)$, and $2\sigma_2^2 \equiv a^2S(am_2,an_2)$. The probability density functions of the single coefficients, being Gaussian, are given by $p(X) = \exp\{-X^2/(2\sigma^2)\}/\sqrt{2\pi\sigma^2}$; $p(Y) = \exp\{-Y^2/(2\sigma^2)\}/\sqrt{2\pi\sigma^2}$.

[3] Temporal and/or spatial averaging can and are in fact often used to smooth the signal spectrum, but not within a single signal transform; several transforms (squared) must be added (incoherently) for different times and/or scatter areas to produce this type of averaging.

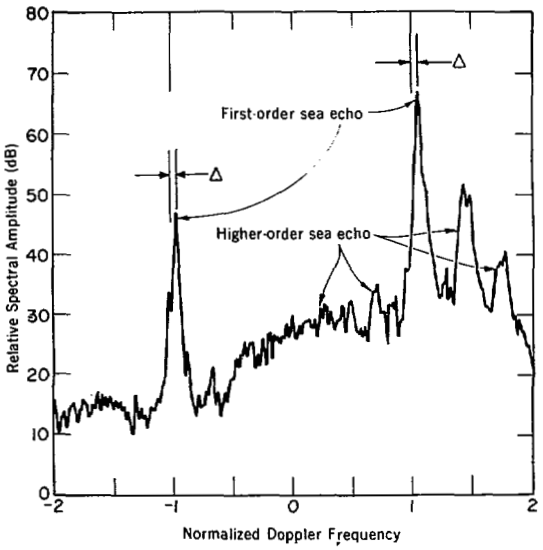

Fig. 1. Typical 9-sample average of 200-s surface-wave HF sea-echo power spectra at 9.4 MHz. Doppler frequency is normalized with respect to expected position of the first-order Bragg peaks (here 0.313 Hz). Δ is the normalized shift of the record due to underlying current.

III. Statistics of the Spectrum for a Gaussian Voltage Signal

In the preceding section we gave a theoretical justification for the hypothesis that the first- and second-order sea-echo voltage signals (and their complex Fourier transforms) are Gaussian random variables. The quantity of interest for extraction of sea-state parameters, however, is the power spectrum of this received voltage signal; hence, our present radar processing equipment outputs this spectrum versus Doppler frequency automatically. Fig. 1 shows an example of a measured nine-sample-averaged surface-wave Doppler spectrum of the sea echo at 9.4 MHz.[4] The specific parameters of the system, and geometry behind this record will be discussed in the next section. The Doppler frequency units of the abscissa are normalized such that 0 corresponds to the carrier position, and ± 1 refers to the predicted positions of the first-order Bragg echo peaks (i.e., $\omega_B/2\pi = \sqrt{2gk_0}/2\pi = \sqrt{g/\pi\lambda} \simeq 0.313$ Hz at a 9.4 MHz carrier). The ordinate is proportional to received power spectral density, and is obtained by taking the sum of the squares of the real and imaginary parts of the digital fast Fourier transform (FFT) output of the receiver. In this case, the FFT was taken on a 200-s coherent echo sample (giving 0.005 Hz Doppler resolution, or 0.016 in the normalized frequency units of Fig. 1). Nine consecutive spectra were averaged (i.e., added together) to produce Fig. 1, the entire figure therefore representing 0.5 h of sea-echo data.

A practical reason for wanting to know whether the received signal is Gaussian has to do with the assessment of error bounds (or confidence) in approximating the true average Doppler spectrum by the average of a finite number of samples. If the signal components are (nearly) Gaussian, such confidences and errors can be readily established, since the required tables for Gaussian statistics are widely available. Hence, we shall establish the variance of the power spectrum for a Gaussian signal in terms of its mean. We shall use this test as an initial indicator of whether the original signal is sufficiently close to Gaussian that further testing is desirable. The further testing will then consist of plotting (on Rayleigh probability paper) the cumulative distribution of the FFT amplitude samples (i.e., the square root of the spectral power); if the original signal were Gaussian, these points should fall along a straight line with a 45° slope.

The sea-echo signal, as represented by (2) and (3) and exemplified in Fig. 1, is a narrow-band zero-mean signal which can be represented in the time domain in the following ways [13].

$$v(t) = A(t)\cos[\omega_0 t + \phi(t)] = \sum_k A_k \cos[(\omega_0 + k\omega_f)t + \phi_k]$$

or

$$v(t) = \frac{2}{T}\sum_k [X_k \cos(\omega_0 + k\omega_f)t - Y_k \sin(\omega_0 + k\omega_f)t] \quad (4)$$

where ω_0 here represents the radian carrier frequency. The latter two forms of the above equation cast the signal in terms of a Fourier series with a fundamental frequency (in the absence of the carrier) of $\omega_f \equiv 2\pi/T$. Following the technique of Rice in Davenport and Root [13], one could allow the period T to become infinite, in which case the series with constant, uncorrelated coefficients could be used to represent a nonperiodic continuous process. Here, however, since in reality a digital FFT treats the process as a Fourier series whose fundamental period T is the window over which the signal is sampled, the last form of (4) is better suited to our purposes.

Following Davenport and Root, we assume that X_k and Y_k are uncorrelated coefficients with zero mean and variance σ_k^2. We shall now determine the variance of the Doppler power spectrum, assuming X_k and Y_k are Gaussian. The output of the FFT for the kth point will be $V(\omega_0 + k\omega_f) = X_k + jY_k$, and we define the power spectrum to be

$$P_k = \frac{|V(\omega_0 + k\omega_f)|^2}{T} = \frac{X_k^2 + Y_k^2}{T}. \quad (5)$$

Since X_k and Y_k are orthogonal by definition (and hence uncorrelated) we have $\langle X_k^2\rangle = \langle Y_k^2\rangle = \sigma_k^2$ and $\langle X_k Y_k\rangle = 0$; because they are Gaussian, all joint moments are the product of the individual moment factors (i.e., $\langle X_k^m Y_k^n\rangle = \langle X_k^m\rangle\langle Y_k^n\rangle$). Using the properties of the Gaussian probability density function, it can be shown that

$$\frac{\langle X_k^4\rangle - \langle X_k^2\rangle^2}{\langle X_k^2\rangle^2} = \frac{\langle Y_k^4\rangle - \langle Y_k^2\rangle^2}{\langle Y_k^2\rangle} = \frac{3\sigma_k^4 - \sigma_k^4}{\sigma_k^4} = 2 \quad (6)$$

[4] Examples of the extraction of sea-state and surface-wind data from such records are found in [7] and [14].

and that P_k is chi-squared-distributed with two degrees of freedom such that

$$\frac{\langle P_k^2\rangle - \langle P_k\rangle^2}{\langle P_k\rangle^2} = 1 \,(\equiv \sigma_p). \tag{7}$$

The latter equation is the desired result, for it gives the (normalized) variance of the individual Doppler power spectral density estimates (about their true mean value) for a Gaussian signal. Any Gaussian signal must have this property, and therefore it is a necessary condition for a Gaussian process (although possibly not sufficient). Since Doppler spectra are the natural output of our existing radar system, we intend to use (7) as a test to determine experimentally whether the signal is Gaussian.

Likewise, higher normalized moments[5] can be established from the general rule $\langle P_k^n\rangle = n!\,\langle P_k\rangle^n$. In this paper, we go no higher than the second—as defined in (7)—for our initial testing. The reason for this is the fact that our experimental sample bases are very small, containing only nine samples per ensemble. (The total number of such separate sample ensemble bases, on the other hand, is five hundred.) When dealing with such a small number of samples per ensemble, higher moments can be expected to become increasingly noisy and thus inaccurate for statistical testing. In general, one can predict that inasmuch as the sea-echo probability density must depart from Gaussian in its tails (since the signal can never approach infinity), these normalized higher empirical moments should fall increasingly short of their predicted values for a true Gaussian process.

The power spectral sample P_k (being the sum of the squares of two uncorrelated Gaussian variables) is predicted to be chi-squared with two degrees of freedom [15]; the probability density for P_k is therefore, the simple exponential function. Hence, the amplitude (i.e., $A_k \equiv \sqrt{P_k}$) of the FFT output is Rayleigh-distributed; this fact will be also employed subsequently for additional statistical testing.

IV. Description of Radar Facility

Sea-state measurements were made by an HF radar located on the west coast of San Clemente Island. The radar system was built by the Institute for Telecommunication Sciences of the Department of Commerce and was operated under contract for the Wave Propagation Laboratory for this series of measurements. Approximately 25 h of data were recorded between December 1972 and April 1973.

Surface-wave radar data were obtained simultaneously at 10 frequencies extending from about 2.4 to 25 MHz. Receiver range gates were set to sample cells centered 22.5, 30.0, and 37.5 km from the radar. The receiving antenna consisted of an array of 13 monopoles phased and switched to alternately produce two beams each having a nominal beamwidth of 10° centered at azimuth angles of 240° and 270°. The combination of 10 frequencies, 3 ranges, and 2 antenna beams resulted in a total of 60 different data samples being recorded.

TABLE I
Summary of San Clemente Island Surface-Wave Radar Characteristics

Operating Frequency Range	2 to 25 MHz
Range Gate Distances	22.5, 30.0, 37.5 km
Available Pulse Lengths	20, 50, 100 μs
	(3.0, 7.5, 15.0 km)
Pulse Repetition Frequency	20 Hz per frequency
Transmitter Peak Power	40 kw
Antenna Beamwidths	
Receiving (2 beams)	10° at 240° and 270° az
Transmitting	60° at 255° az
Antenna Gain Product	18 dB at center of HF band decreasing to 0 dB at band edges

The transmitting antenna was a two-bay, vertically polarized log-periodic antenna having a nominal half-power beamwidth of 60° over the HF band. Since this beamwidth illuminated both sectors covered by the receiving beams, no transmitter antenna steering was used. Power patterns of both receiving and transmitting antennas were measured from a small boat to verify gain and beamwidth performance. Radar characteristics are summarized in Table I.

An on-line computer processed the received signals and computed the power spectrum for each of the 60 data channels. The power spectra which were processed on-line were calculated from signals that had been coherently sampled over a 200-s window. Since a typical measurement period was 30 min, a total of 9 spectra would be computed during this time. These power spectra and the unprocessed IF data were recorded on magnetic tape to permit subsequent analysis of the raw data.

V. Measured Sea Echo Properties

A. Standard Deviation of Spectral Peaks

The normalized standard deviation σ_p of the power at the spectral peaks was computed for power spectra having coherent integration times of 200 s. Thus, the quantity σ_p for a 30-min sample represents the standard deviation of $N = 9$ spectral peaks divided by the average maximum of the 9 spectra in the sample. Normalized standard deviations were calculated for both the absolute maxima of the spectra in the vicinity of the first- and second-order Bragg frequencies and for the spectral power at constant Doppler frequencies near $\pm f_B$ and $\sqrt{2}\,f_B$. The Bragg frequency f_B is defined as $f_B = \omega_B/2\sqrt{g/\pi\lambda}$.

The data studied consisted of approximately 7½ h of measurements for a wide variety of sea states with significant waveheights ranging from 1 to 4 m (wave characteristics were measured by a Waverider Data Buoy moored 29.4 km from the radar site on an azimuth of 240°); 500 individual spectra have been considered in our analysis. Mean values of σ_p versus range are listed in Table II for the different spectral lines. We see there is no systematic tend of σ_p with

[5] The nth normalized moment is defined as
$$\langle (P_k - \langle P_k\rangle)^n\rangle / \langle P_k\rangle^n.$$

TABLE II
MEAN NORMALIZED STANDARD DEVIATIONS AT DIFFERENT RANGES FOR ABSOLUTE MAXIMA AND SPECTRUM AT FIXED DOPPLER FREQUENCY

Doppler Line	Range			All Data Combined
	22.5 km	30.0 km	37.5 km	
	Fixed Doppler near Maxima			
1 +	0.912	0.917	0.918	0.916
1 -	0.921	0.930	0.974	0.942
2 +	0.948	0.954	0.954	0.952
	Absolute Maxima			
1 +	0.736	0.719	0.707	0.720
1 -	0.740	0.712	0.675	0.709
2 +	0.496	0.468	0.485	0.483

Note: 1 + and 1 - are first-order advancing and receding lines near f_B; 2 + is the second order advancing line near $\sqrt{2}\, f_B$

TABLE III
NORMALIZED STANDARD DEVIATIONS FOR TWO PULSE LENGTHS TRANSMITTED DURING ADJACENT 30-MIN PERIODS

Doppler Line	Range			All Data Combined
	22.5 km	30.0 km	37.5 km	
	Fixed Doppler - 20 μs Pulse			
1 +	0.816	0.876	1.024	0.905
1 -	0.927	0.990	0.947	0.955
2 +	0.929	0.940	0.886	0.918
	Fixed Doppler - 100 μs Pulse			
1 +	0.972	0.859	0.928	0.920
1 -	0.951	0.901	0.891	0.914
2 +	0.878	0.966	0.913	0.919
	Absolute Maxima - 20 μs Pulse			
1 +	0.659	0.796	0.733	0.729
1 -	0.719	0.861	0.646	0.742
2 +	0.502	0.442	0.515	0.486
	Absolute Maxima - 100 μs Pulse			
1 +	0.786	0.747	0.737	0.757
1 -	0.735	0.772	0.732	0.746
2 +	0.506	0.414	0.466	0.462

range, and hence none with cell size. Similarly, no dependence of σ_p with operating frequency was observed. The normalized standard deviation is slightly less than unity for the spectra at a fixed Doppler frequency indicating that the Gaussian model is approximately correct. The ratio is about 0.71 for the absolute power maxima of first order peaks; no model has yet been pursued which explains this result. The second-order average for the absolute maxima is about 0.5, indicating that perhaps still a different model applies to this spectral line.

As a further check of possible dependence of σ_p on range cell size, two pulse widths (20 and 100 μs) were transmitted for consecutive 30-min periods, during which significant waveheight and direction remained fairly constant. The normalized standard deviations obtained at each pulse length are shown in Table III. We see that the results for different pulse lengths are not significantly different from the values obtained for all data combined. Therefore, we conclude that there is little, if any, dependence of σ_p upon cell size.

The correlation coefficient between normalized standard deviation and significant waveheight during the sample period was computed to determine whether the quantity σ_p can be used as a predictor of sea state. Since the observed correlation values were not statistically significant, we must conclude that σ_p is *not* a useful indicator of sea state.

B. Cumulative Distributions of Measured Data

The measured standard deviations σ_p for the spectral power at fixed Doppler frequency are sufficiently close to the predicted values for a Gaussian process (i.e., 0.916, 0.942, and 0.952 compared to unity) that further statistical testing is desirable. This is especially true since the theoretical analyses of Section II predict Gaussian processes. No further testing will be done, however, on the spectral data at the absolute spectral maxima, since the normalized standard deviations are quite different from Gaussian predictions (0.720, 0.709, and 0.483 compared to unity). Furthermore, no simple model (with a minimum of undetermined parameters) exists which can shed light on this spectral statistic; hence, it will not be examined further in this paper.

As an additional check to establish the Gaussian nature of HF sea echo, we examined the distribution of spectral power at a fixed Doppler frequency. From Section III, the FFT amplitude should be distributed according to the Rayleigh distribution if the echo signal is a Gaussian random variable. Therefore, our second test consisted in determining whether the spectral amplitude recorded over a period when the sea was statistically stationary was Rayleigh-distributed.

To obtain an adequate sample size, we calculated 72 spectra with 25-s integration time from continuous IF sea-echo data recorded over a 30-min period. First- and second-order ($\pm f_B$ and $\sim\sqrt{2}\, f_B$) data points were sorted into 0.5-dB intervals for computation of cumulative distributions of spectral amplitude. The distributions were expressed in decibels and plotted on special "Rayleigh-distribution" graph paper. This paper is constructed such that a Rayleigh-distributed variable will fall along a straight line having a slope of -1.

Fig. 2 shows the result for the first-order advancing and receding Bragg lines. The data points are the cumulative distributions obtained at three operating frequencies; the solid lines indicate the slope which a Rayleigh-distributed quantity would have. Except for some departures in the higher percentage tails, the data points appear to fall along straight lines having the slope criterion required for the Rayleigh distribution.

Data for the second-order approaching lines at the same three frequencies are plotted in Fig. 3. Again, the solid line shows the slope characteristic of a Rayleigh-distributed quantity. Although there appears to be a somewhat larger

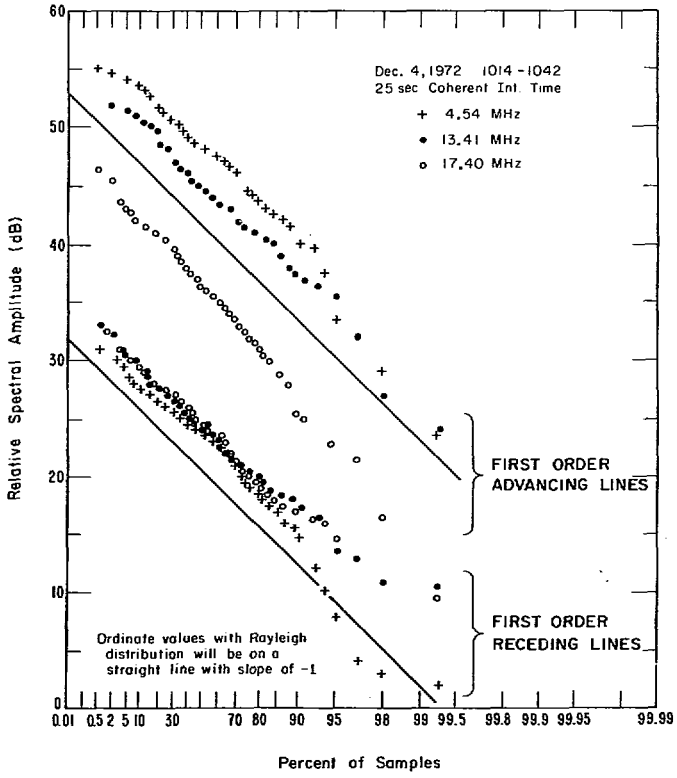

Fig. 2. Cumulative distribution of spectral amplitudes at fixed Doppler frequency ($\pm f_B$) for three sets of 72 spectra. Solid lines indicate slope = −1.

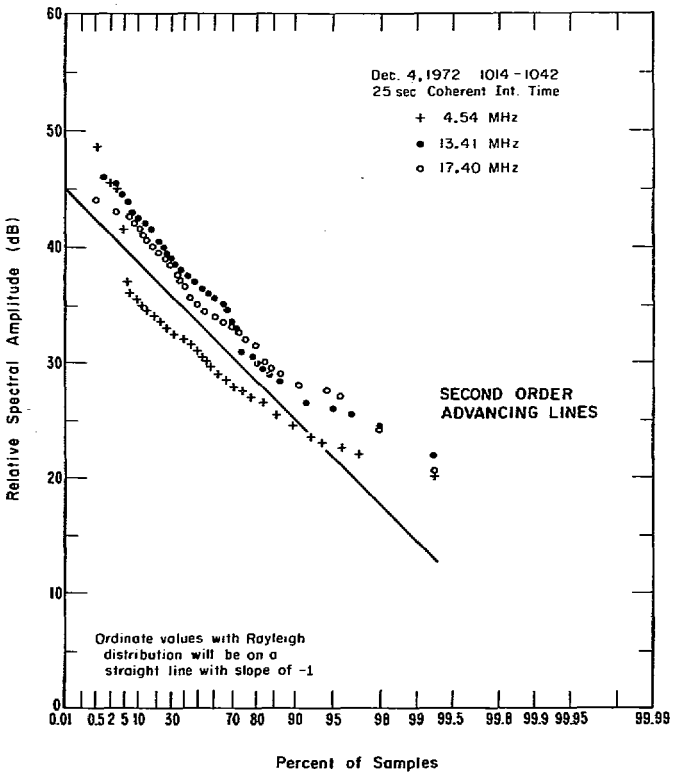

Fig. 3. Cumulative distribution of spectral amplitudes at fixed Doppler frequency ($\sqrt{2}\,f_B$) for three sets of 72 spectra. Solid line indicates slope = −1.

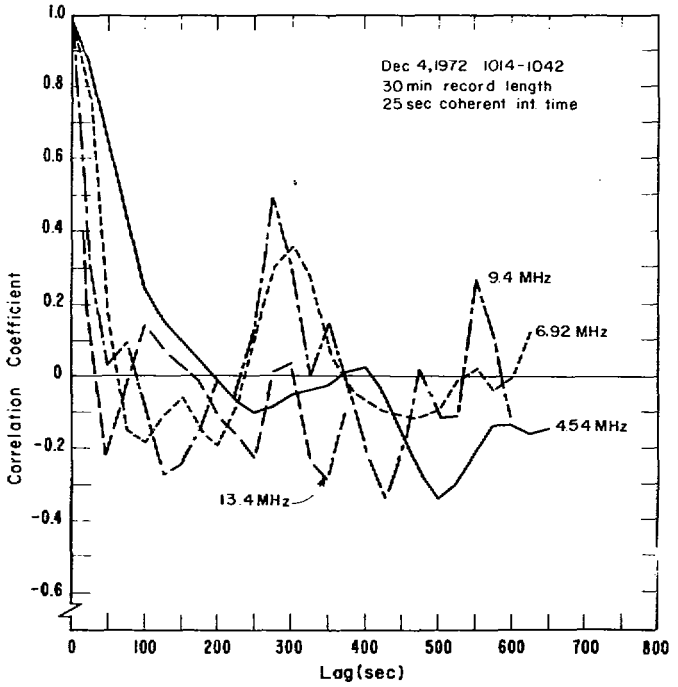

Fig. 4. Autocorrelation of first-order advancing maxima versus operating frequency.

departure from a straight line than was observed for the first-order lines, the data points have nearly the required slope.

We consider the apparent Rayleigh-distribution of spectral amplitudes at fixed Doppler frequency as additional confirmatory evidence that HF sea echo is described reasonably well by a Gaussian process.

C. *Autocorrelation of Spectral Peaks*

To determine the time between independent samples and the associated implications as to optimum measurement periods, we computed the autocorrelation $\rho(\tau)$ of first- and second-order portions of the power spectrum. This quantity is the correlation between spectral peaks separated by integral multiples of the coherent integration time; thus the autocorrelation is computed for lags τ equal to nT, $1 < n < N - n$, where T is the coherent integration time and N is the total number of spectra in the record length. We made calculations for coherent integration times of 25, 50, 100, and 200 s; the total record length was 30 min. As in the case of the normalized standard deviation, calculations were performed for both absolute peaks and power near these peaks but occurring at a constant Doppler frequency. Because of the fairly large amount of computer time required, only two sea states were considered. The first sample had a significant waveheight ($H_{1/3}$) of 1.5 m while the second had $H_{1/3} = 4$ m.

In Fig. 4 we present $\rho(\tau)$ observed on December 4, 1972 ($H_{1/3} = 1.5$ m) for the first-order advancing line. This result is very similar to that observed during the period with $H_{1/3} = 4$ m; thus, over the range of significant waveheights used in this analysis, waveheight does not appear to affect

TABLE IV
TIME REQUIRED FOR CORRELATION COEFFICIENTS TO DECREASE TO $1/e$ (0.368). RANGE = 22.5 KM; PULSEWIDTH = 50 μS. DATA TAKEN DECEMBER 4, 1972, 1014–1042 PST

Frequency	Time(s) Absolute Maxima			Fixed Doppler Maxima		
(MHz)	+ 1	- 1	+ 2	+ 1	- 1	+ 2
2.41	140	65	*	140	25	*
4.54	85	40	*	80	55	*
6.92	35	35	35	30	40	20
9.40	20	30	20	20	20	20
13.41	20	20	15	25	20	20

* There is no well defined second order component at this frequency

the correlation between spectral peaks for the predominant line. In addition, for the first-order advancing lines, the "correlation function" is very similar for both the absolute peaks and for the spectra at a fixed Doppler. However, the first-order receding and second-order advancing lines show a much more rapid decrease in correlation coefficient with lag time; in fact, the spectral peaks are uncorrelated after a single lag period of 25 s.

For the first-order advancing line, the correlation at the lower operating frequencies decreases more slowly than at higher frequencies. At frequencies greater than about 7 MHz, all these major spectral components are uncorrelated after a single lag interval. To show the behavior of the correlation coefficient of the spectral lines with frequency, in Table IV we tabulate the time required for the correlation coefficient to decrease to $1/e$. These values were obtained for a coherent integration time of 25 s. Since the correlation does not change significantly with range, data for only a single range are given.

When considering the correlation results for the longer coherent integration times, we find little difference in the general shape of the correlation function. Although some detail is smoothed out at the longer integration times, it is clear that there is no important difference in $\rho(\tau)$ for either a 25 or 50 s time interval. At 100 and 200 s integration times, sufficient detail is lost that comparison with the shorter times is difficult. However, to generalize the results at these longer times, we find that the peaks are uncorrelated after a single lag period at all frequencies.

The fact that spectral peaks at higher frequencies are largely uncorrelated after 25 s has important implications for over-the-horizon (OTH) sensing of sea state. Since higher frequencies are likely to be used in the OTH work, especially at the longer ranges, independent samples would be obtained with a 25 s coherent integration time. This is fortunate since the ionosphere is unlikely to remain stable for much longer periods. For sea-state sensing using an HF surface-wave radar, independant samples are always obtained using coherent integration times of 200 s.

A possible physical interpretation of the observed time between independent spectral samples can be deduced by noting that this time is approximately the reciprocal of the width of the respective spectral peak (measured in hertz) at which the correlation time was measured. Meteorologists have established this relationship for radar spectra of rain echoes [16], [17]. The explanation for the spectral peak widths in that case relates to the differential raindrop fall velocities, and how long it takes for two typical raindrops with different velocities to produce a scattered signal phase change of 180°. The corresponding explanation for first-order scatter from the sea, for example, would suggest that the reciprocal of the first-order spectral peak width is essentially the time it takes for two typical periodic Bragg-scattering ocean wavetrains (within the resolution cell)—but having slightly different velocities—to slide one-half wavelength with respect to each other.

VI. SAMPLE EXTRAPOLATION TO SYSTEM DESIGN

The statistical analyses of the HF sea-echo signal undertaken in the previous sections have application to system design. The two results which are most immediately useful are the facts that i) the narrowband time signal is (approximately) Gaussian, and ii) the time between independent spectral samples is ~25–50 s over most of the HF region.

As an example, plans are underway to construct and operate a skywave research radar on San Clemente Island for sea-echo observations. Due to antenna scan time, a Doppler spectrum can be constructed for a given ocean patch only every T_s s (for the San Clemente Island skywave radar planned for the Gulf of Alaska observations, one mode of operation has $T_s \simeq 500$ s, with a coherent integration time per spectrum of 25 s). Since T exceeds 50 s, each spectrum is uncorrelated and independent of all others, according to the results of the preceding section. In order to extract average sea-state data from the echo, an "average" Doppler power spectrum must be constructed. This "average" is actually the sum of N independent spectral samples taken T_s s apart. An ensemble average—in which the spectrum fluctuations vanish as the spectrum approaches its true mean—is obtained as N approaches infinity. However, one cannot generally afford to wait this long; 1 or 2 h may be the practical upper limits of desirable system operation, due both to operating costs and also to the fact that sea state can change after several hours, making the statistics "nonstationary." During 1 h, for example, where $T_s \simeq 500$ s, only about $N = 7$ independent samples would be used to form the "average." This therefore is not a true "average" power spectrum, but is itself a random sample fluctuating about the true mean. The greater N, the less the fluctuation of the "sample average," and hence the less error involved in estimating the desired sea-state parameters. Thus one has the trade-off between reducing statistical errors in the desired output data versus requiring too much time to gather the data, with the resulting question—what is the optimum or "break-even" point in terms of the total number of independent samples, N (or the total data collection time NT_s)?

If one cannot assume Gaussian statistics, there is nothing one can do short of a massive program of gathering data and extracting empirical results. Since we can assume that the signal here is Gaussian, we can readily derive errors and

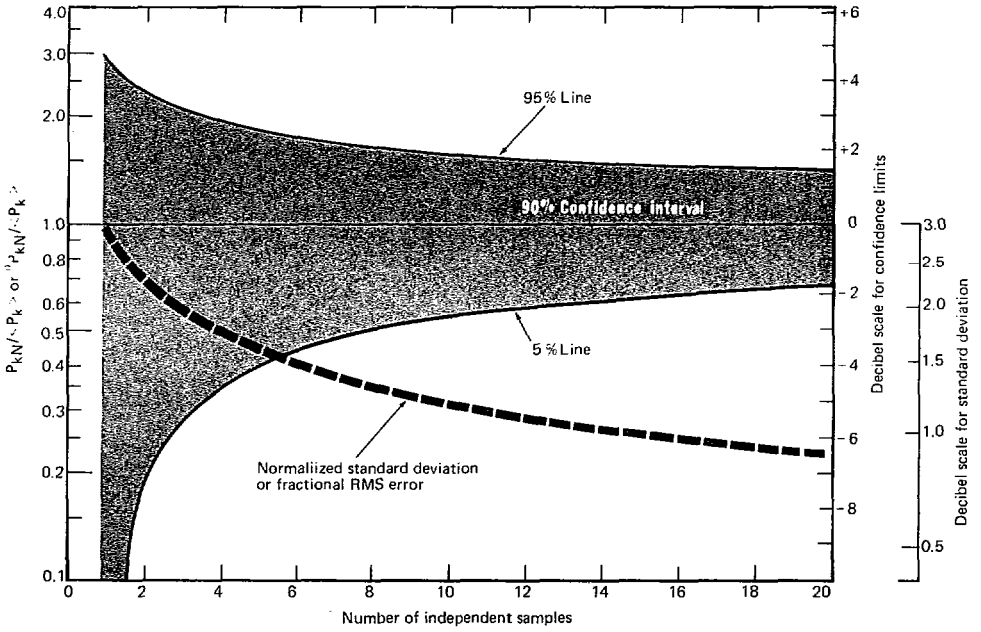

Fig. 5. Normalized standard deviation and 90 percent confidence interval for power spectra of Gaussian process versus number of independent samples.

confidence limits of the power spectrum versus the number of independent samples. Let us define P_{kN} as the sample average over N independent samples, with $\langle\cdot\rangle$, as before, signifying the true average over an infinite ensemble. We define the variance of the sample average as

$$\begin{aligned}\sigma_{P_{kN}}^2 &= \langle P_{kN}{}^2 - \langle P_{kN}\rangle^2\rangle \\ &= \left\langle \left[\frac{1}{N}\sum_{n=1}^{N}\frac{X_{kn}{}^2 + Y_{kn}{}^2}{T}\right]\right\rangle^2 - P_k{}^2 \\ &= \frac{1}{T^2N^2}\left[\sum_{n=1}^{2N}\langle X_{kn}{}^4\rangle \right. \\ &\quad \left. + \sum_{m=1}^{2N}\sum_{n=1}^{2N}\langle X_{km}{}^2\rangle\langle X_{kn}{}^2\rangle - (2\sigma_k{}^2)^2\right]. \end{aligned} \quad (8)$$

Noting that X_{kn} and Y_{kn} have the same (Gaussian) distribution, and are uncorrelated, we arrive at the following answer for the (normalized) variance and standard deviation (or fractional rms error) in the spectral average of N samples:

$$\sigma_{P_{kN}}^2/\langle P_k\rangle^2 = 1/N \quad \text{or} \quad \sigma_{P_{kN}}/\langle P_k\rangle = 1/\sqrt{N}. \quad (9)$$

The latter normalized standard deviation is shown plotted in Fig. 5, both on an absolute scale and in decibels. By multiplying the abscissa by T_s (the time between samples), one has a measure of the fractional rms spectral error versus operating time.

Another measure of the quality of an average of N independent samples is the confidence interval. This can be found by noting that since X_{kn} and Y_{kn} have the same statistics but bare uncorrelated, one can write

$$P_{kN} = \frac{1}{N}\sum_{n=1}^{N}\frac{(X_{kn}{}^2 + Y_{kn}{}^2)}{T} = \frac{1}{NT}\sum_{n=1}^{2N}X_{kn}{}^2. \quad (10)$$

Now, since X_{kN} is Gaussian, it is true that NP_{kN} is chi-squared with $2N$ degrees of freedom (see for example Hogg and Craig [15]). Thus one can use the standard tables for this distribution to estimate the confidence. A 90 percent confidence interval for $P_{kN}/\langle P_k\rangle$ is shown in Fig. 5 for the power spectral average consisting of N samples. The upper and lower limits are set symmetrically so that 5 percent of the points will fall above the upper line and 5 percent below the lower line. Therefore, the shaded zone represents the region (for given N) where 90 percent of the "average" spectral estimates P_{kN} will fall.

From both sets of curves, one can see for example that increasing the averaging time from 1 to 2 h (where T_s = 500 s) will decrease the rms error from 1.4 to 1.0 dB, and will decrease the total 90 percent confidence spread from 5.57 to 3.87 dB. This decrease in the statistical error may be considered marginal in terms of operating costs for the additional hour for certain applications.

VII. Conclusions

Our investigation into the statistics of HF sea scatter observed at San Clemente Island has revealed the following facts.

1) The first- and second-order portions of the received echo signal voltage are described reasonably well by a Gaussian process. This empirically implies that the sea wave-height is nearly Gaussian, a fact which has been ascertained and known to oceanographers for many years. Consequences of this result are the facts that i) the normalized standard deviation of the echo power at any given spectral frequency is unity and ii) the amplitude (square-root of power) at any given spectral frequency is Rayleigh-distributed.

2) The normalized standard deviation of the maximum of the first-order power spectral peak (which wanders slightly in frequency from record to record), on the other hand, is observed to be 0.7. The same quantity for the second-order peak is observed as ~ 0.5. While it is physically reasonable that these standard deviations should be less than unity, we presently have no satisfactory model which explains these results quantitatively.

3) The normalized standard deviations observed above appear from the data to be independent of range, radar resolution cell size, radar operating frequency, and sea state (i.e., significant waveheight).

4) The autocorrelation function (versus time) of the power spectra appears to be independent of sea state (i.e., waveheight) and cell size, but is slightly dependent upon radar operating frequency below 7 MHz. Above 7 MHz, the power spectra are essentially uncorrelated after 25 s. The heretofore accepted explanation that the correlation time should be roughly the time it takes the scattering wavetrains to pass through the cell (e.g., ~ 1550 s for a 7.5-km cell size at 10 MHz) is entirely inadequate to explain our observations. A more likely explanation relates this time to the reciprocal of the width of the respective spectral peak: this latter quantity in turn can be related to the differential velocities between the scattering ocean wavetrains, which resembles a "turbulence" phenomenon.

5) The implication of the previous result is that uncorrelated samples of sea-echo power spectra are obtained for intervals greater than 25 s in the upper HF band (where a skywave OTH radar would normally operate). This fact—combined with the Gaussian nature of the sea echo also established herein—makes it possible to predict the statistical errors inherent in spectral samples of finite number. For example, a power spectral average of 14 independent samples was shown to have an rms error (or fluctuation) about the mean of 1.0 dB.

References

[1] D. D. Crombie, "Doppler spectrum of sea echo at 13.56 Mc/s," *Nature*, vol. 175, pp. 681–682, 1955.
[2] J. R. Wait, "Theory of HF ground wave backscatter from sea waves," *J. Geophys. Res.*, vol. 71, pp. 4832–4839, 1966.
[3] D. E. Barrick and W. H. Peake, "A review of scattering from surfaces with different roughness scales," *Radio Science*, vol. 3, pp. 865–868, 1968.
[4] D. E. Barrick, "First-order theory and analysis of MF/HF/VHF scatter from the sea," *IEEE Trans. Antennas Propagat.*, vol. AP-20, pp. 2–10, 1972.
[5] ——, "Remote sensing of sea state by radar," in *Remote Sensing of the Troposphere*, V. E. Derr (Ed.), U.S. Government Printing Office, Washington, DC: 1972, ch. 12.
[6] A. E. Long and D. B. Trizna, "Mapping of North Atlantic winds by HF radar sea backscatter interpretation," *IEEE Trans. Antennas Propagat.*, vol. AP-21, pp. 680–685, 1973.
[7] D. E. Barrick, J. M. Headrick, R. W. Bogle, and D. D. Crombie, "Sea backscatter at HF: Interpretation and utilization of the echo," *Proc. IEEE*, vol. 62, pp. 673–680, 1974.
[8] G. V. Trunk, "Radar properties on non-Rayleigh sea clutter," *IEEE Trans. Aerospace and Electronics Syst.*, vol. AES-8, pp. 196–204, 1972.
[9] A. Papoulis, "Narrowband systems and Gaussianity," *IEEE Trans. Inform. Theory*, vol. IT-18, pp. 20–27, 1972.
[10] ——, *Probability, Random Variables, and Stochastic Processes*. New York: McGraw-Hill, 1965, p. 583.
[11] S. O. Rice, "Reflection of electromagnetic waves from slightly rough surfaces," *Theory of Electromagnetic Waves*, M. Kline, Ed. New York: Interscience, 1961, pp. 351–378.
[12] B. Kinsman, *Wind Waves*. Englewood Cliffs, NJ: Prentice-Hall, 1965, p. 676.
[13] W. B. Davenport, Jr., and W. L. Root, *An Introduction to the Theory of Random Signals and Noise*. New York: McGraw-Hill, 1958, p. 393.
[14] J. L. Ahearn, S. R. Curley, J. M. Headrick, and D. B. Trizna, "Tests of remote skywave measurement of ocean surface conditions," *Proc. IEEE*, vol. 62, pp. 681–687, 1974.
[15] R. V. Hogg and A. T. Craig, *Introduction to Mathematical Statistics*. New York: Macmillan, 1959, p. 245.
[16] R. M. Lhermite, "Motions of scatterers and the variance of the mean intensity of weather radar signals," Sprery Rand Res. Center Program 38310, Rept. No. SRRC-RR-63-57, Atmospheric Physics Dept., Sudbury, MA, 1963.
[17] F. E. Nathanson, *Radar Design Principles*. New York: McGraw-Hill, 1969.

Studies of Backscattered Sea Return with a CW, Dual-Frequency, *X*-Band Radar

WILLIAM J. PLANT

Abstract—**A coherent, CW, dual-frequency, *X*-band radar was used to study microwave sea return from the Chesapeake Bay. It is shown that the product of the backscattered fields depends strongly on long surface wave properties. In particular, a sharp line is found in the product power spectrum whose frequency is that of the water wave whose wavelength is in resonance with the spatial period of the beat frequency between the two transmitted signals and whose wave vector is parallel to the horizontal line of sight. Thus, gravity wave dispersion relations can be obtained with the system. Furthermore, the degree of modulation of short waves by long ones is given by the intensity of the line. A broad background corresponding to the convolution of the single-frequency Doppler spectra is also seen in the product power spectrum. These**

Manuscript received August 28, 1975; revised January 15, 1976.
The author is with the Naval Research Laboratory, Washington, DC 20375.